Extreme sea levels in Guam: Incorporation of wave-driven setup and runup into the analysis of fluctuations in extreme high waters at the Ipan reef

A thesis submitted to the global environmental science undergraduate division in partial fulfillment of the requirements for the degree of

bachelor of science

in

global environmental science

December 2012

By Sarah Yasui

Thesis Advisor:
Mark Merrifield

Abstract

Changes in mean sea levels influence the coast by affecting the height and frequency of extreme high waters. Tide-gauge records are often used to study fluctuations in the timing and severity of extreme sea levels because these records are relatively long and accessible. However, there are two main limitations to analyzing sea-level extremes using tide-gauge observations: 1) Tide gauges are often protected from wave energy, and therefore do not account for the elevation of water levels due to setup, and 2) instruments with sampling frequencies of several minutes to an hour may not correctly identify the most extreme sea level. Here it is found that sea-level extremes documented by tide gauges at Pago Bay and Apra Harbor, located in eastern and western Guam, respectively, differ significantly in height when the observations are evaluated alongside a high-frequency (1 Hz) sea-level record from Ipan that has been modified to include the influences of setup and extreme runup. The disparity between water levels with and without wave effects is especially pronounced (as high as 1.5 m) during large wave events (>2 m). Extreme high waters appear to be correlated to a surge in southwesterly monsoon winds in Apra Harbor and the passage of tropical cyclones close to (<370 km) the island in Pago Bay and Ipan. The sea-level response to the passage of a tropical cyclone over Guam does not appear to be correlated to storm intensity or proximity.

Contents

List of Tables

List of Figures

1 Introduction

1.1 Sea-level extremes

Although mean sea level variations constitute the focus of a rich collection of research, it is the fluctuations in the height and frequency of extreme sea levels that directly influence the coastal zone (Bindoff et al., 2007). Extreme sea-level events are rare but hazardous episodes typically associated with tropical or extratropical storms (e.g., typhoons). Extreme high waters can damage coastal infrastructure and threaten the safety of coastal inhabitants through inundation and/or erosion. The ability to project the timing, frequency, and severity of extreme sea levels is crucial for disaster management because such predictions allow for the development of appropriate setbacks for construction of coastal infrastructure, establishment of maritime safety, etc.

The destructive potential of extreme sea-level events can be augmented if the timing of an intense storm or large swell coincides with spring tides (Menendez et al., 2009), which are tides of increased range that accompany the occurrence of a new or full moon approximately twice per month. In addition to tides, modes of climate oscillation, such as the El Niño Southern Oscillation (ENSO), and periodic tidal modulations, namely the 4.4-year quasi-nodal cycle and 18.6-year perigean tides, also influence the timing and severity of extreme sea levels (Menendez et al., 2009; Menendez and Woodworth, 2010; Mendez et al., 2006; Haigh et al., 2010). Menendez et al. (2009) developed a statistical model that incorporates the varying temporal (seasonal, interannual, and secular) and tidal (nodal cycle and perigean tides) elements of sea levels to predict the probability of incidence of extreme high waters. Thus, regional variability in extremes appears to be a manifestation of seasonal (e.g., spring tides, storm seasons), interannual (e.g., El Niño Southern Oscillation, North Atlantic Oscillation), decadal (e.g., Pacific Decadal Oscillation), and secular (e.g., sea-level rise) sea surface height fluctuations (Woodworth and Blackman, 2004; Mendez et al., 2006; Menendez et al., 2009; Menendez and Woodworth, 2010). The extent to which these components affect regional extremes varies temporally and spatially.

Changes in the frequency and/or severity of sea-level extremes can have disastrous impacts on vulnerable coastal zones; the authors of numerous studies have detected an increase in the frequency of extreme sea levels within the past several decades. Woodworth and Blackman (2004) found an increase in the frequency of extremes since 1975 by analyzing sea-level data obtained from a nearly global array of 141 tide gauges. They attribute this observation to interannual and secular trends in mean sea level. Menendez and Woodworth (2010), also utilizing data from a quasi-global distribution of tide gauges, observed a worldwide increase in

high-water levels since the 1970s, with a greater rate of increase observed within more recent decades than for the 20th century overall. Their analysis revealed that the variations in high water levels depends principally on secular changes in mean sea level; positive trends in extremes were virtually eliminated upon the removal of annual mean sea levels from the tide-gauge records. Menendez and Woodworth (2010) also found that tidal modulations (nodal cycle and perigean tides), seasonal factors (spring tides and storm seasons), and climate oscillations (particularly ENSO) affected the observed fluctuations in extremes, but to a much lesser extent than mean sea level changes. By analyzing the Honolulu Harbor tide-gauge record spanning from 1918-2003, Firing and Merrifield (2004) associated the increase in the frequency of sea-level extremes in recent decades to a long-term increase in mean sea level. They found that extreme events in Honolulu display a 20-year periodicity associated with interdecadal sea-level fluctuations. Marcos et al. (2009) analyzed data from 73 tide gauges and observed that interannual fluctuations in extreme sea levels along the Atlantic and Mediterranean coasts of southern Europe were negatively correlated with the winter North Atlantic Oscillation (NAO) index. Increasing trends in extreme sea levels observed at the Atlantic tidal stations appeared to be driven mean sea level changes (as opposed to changes in storminess). Haigh et al. (2010), by using sea level records from 18 tide gauges within the English Channel, detected an increase in the frequency of sea-level extremes since the 20th century, but not at a rate statistically different from the increase observed in mean sea levels. Fluctuations in extremes were linked to mean sea level variability, the 18.6-year nodal tidal cycle, and regional climate oscillations (particularly the NAO). Bromirski et al. (2003) found evidence for an increase in extreme non-tidal residual sea levels (with a greater rate of increase since 1950) in San Francisco, California, where a long, 140-year tide-gauge record spanning from 1860-2000 is available. The authors of this study also observed similar periods in the residual sea-level record characterized by elevated levels of extremes and suggested the current increasing trend will not likely persist; recent fluctuations in extremes were attributed to increases in storminess.

The authors of some studies have detected negative trends in the frequency of extreme sea levels. For instance, Bernier and Thompson (2006), using tide-gauge records and a 40-year hindcast of storm surges from the east coast of Canada and the northeastern U.S., linked the slightly negative trend in the frequency of extremes over most of the northwest Atlantic between 1960 and 1999 to changes in atmospheric pressure minima.

In summary, the fluctuations observed in the magnitude and frequency of extreme sea levels appear to be influenced by 1) secular changes in mean sea level, 2) natural climate variations, and 3) the nodal and perigean tidal cycles. Changes in the frequency and/or intensity of storms can also affect extreme-event

dynamics. Bromirski et al. (2003) (as well as Graham and Diaz (2001), to be discussed in the following section) found evidence for an increase in storminess.

1.2 Changes in wave heights

An increasing trend has been observed in the frequency of extreme wave heights in the Pacific northeast. The majority of authors who studied the trends in extremes within this region attribute the fluctuations in wave heights to natural climate variations. Allan and Komar (2000), by using 20-30 year records of wave data from six buoys along the Eastern North Pacific from the Gulf of Alaska to northern California, linked the increase in winter wave heights and periods within the past few decades to regional climate variability associated with ENSO and the East Pacific Pattern. Graham and Diaz (2001), by analyzing cyclone statistics and measured and hindcast wave data for the central North Pacific, attributed the increase in the frequency and intensity of winter cyclones and extreme wave heights since the mid-20th century to intensification of upper-tropospheric winds, a trend that may be related to natural climate variations or increased sea-surface temperatures in the western tropical Pacific. Menendez et al. (2008) also detected an increase in the magnitude of extreme wave heights in the Pacific Northeast (especially off of the coasts of Washington, Oregon, and California) by utilizing hourly significant wave height data from 26 NOAA and Environment Canada buoys from 1985-2007. The observed trends were linked to the Pacific/North American teleconnection pattern (PNA) and ENSO. Ruggiero et al. (2010) analyzed hourly deep-water significant wave heights from buoys along the Oregon and Washington coasts and found that annual average significant wave heights have been increasing at a rate of approximately 0.015 m yr^{-1} since the mid-1970s.

1.3 Wave setup and runup

Fluctuations in extreme sea levels are typically analyzed using tide-gauge records, which constitute the longest type of sea-level data available to researchers on a global scale. However, wave influences, particularly setup and runup, are generally not incorporated into such analyses; to the authors knowledge, the research performed by McInnes et al. (2009) on extreme high waters in southeastern Australia constitutes the only study addressing wave-driven effects on the prediction of extreme sea levels thus far. Wave setup is the time-averaged elevation of the sea surface height from the breaker zone to the shoreline driven by the shoreward flux of momentum from the open ocean to the coast in the form of waves (see Figure 1). Swash (the fluctuation about the elevated water levels) is the time-varying location of the intersection between the ocean and the beach. Runup consists of the contributions of both setup and swash; extreme runup in this

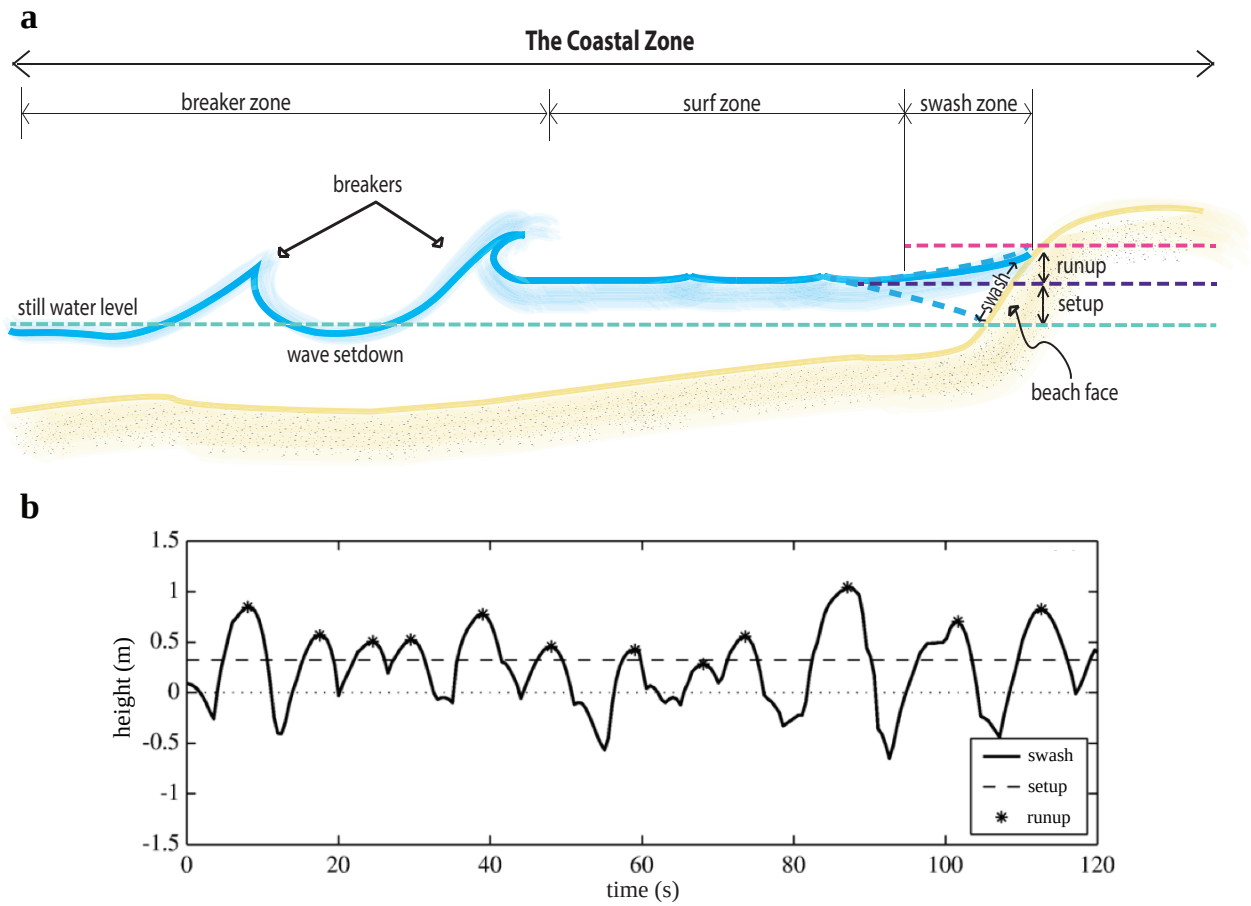

Figure 1: **a** Schematic highlighting features of the nearshore zone. Definitions of setup, swash, and runup are adopted from Stockdon et al. (2006). **b** A plot of setup, swash, and runup adapted from Stockdon et al. (2006).

study is defined as water levels that surpass a particular threshold. These definitions correspond to those used by Stockdon et al. (2006). During extreme sea-level events, wave-driven surge transfers the energy from large ocean waves to the shoreline, potentially eroding beaches, damaging coastal infrastructure, and causing inundation.

tide-gauge observations are generally referenced to a tidal datum, a standard elevation delineated by a particular phase of the tide. Mean sea level (MSL), the averaged hourly tidal heights for a period of at least a year, and Mean Lower Low Water (MLLW), the average of the lower low water levels in a tidal day, are frequently used as tidal benchmarks (Pugh, 1987). The still water level (SWL) consists of the height contributions from mean sea level, the tides, and surge effects, but excludes the influence of waves on water levels; swells propagate above the SWL (see Figure 1).

The protected nature of tide gauges makes it difficult to incorporate wave-driven effects into studies of extreme sea levels. Tide gauges were effectively designed so that one can distinguish the long-term sea-level fluctuations from shorter-period variations associated with local weather patterns and wave activity (Pugh, 1987). Therefore, tide gauges are not generally situated in coastal areas exposed to wave energy or strong currents, both of which can produce significant sea-surface height gradients; these instruments are instead situated in areas sheltered from wave energy (i.e., bays or harbors) or seaward of the breaker zone (Pugh, 1987).

The incorporation of wave effects into extreme-event projections is also difficult because of the lack of long-term, high frequency sea-level data available to researchers on a global scale (Woodworth, 2006). Most of the instrumentation designed to record sea level, such as tide gauges, have sampling frequencies of several minutes to an hour (or greater) so that wave impacts on sea level become averaged into the measurements. Higher-resolution topographic, bathymetric, and atmospheric datasets would also likely be required to accurately model setup and runup (McInnes et al., 2009).

An empirical parameterization of extreme runup, developed by Stockdon et al. (2006) using runup data collected from North Carolina, California, Oregon, and the Netherlands in a wide range of wave conditions, requires only the input of the foreshore beach slope, offshore wave height, and deep-water wavelength in order to predict extreme runup heights for a particular coastline. However, this empirical expression does not work as well for the study site considered here (and probably for similar types of reef environments) as it may for other beach varieties.

Despite these limitations, it is apparent that the study of wave-driven impacts on extreme sea-level fluctuations is crucial to effective coastal management because it is only through a comprehensive understanding of past high-water trends that researchers will be able to accurately predict the timing, frequency, and severity of such events in the future. The objectives of this study are to determine water levels including wave-driven setup and runup heights and to analyze how these wave effects influence water levels at the Ipan reef on southeastern Guam. Though there may also be some disparity between the distribution of extreme events between sea-level records with and without wave influences, the water level record from Ipan (roughly 5 years) is not long enough to perform such an analysis.

1.4 The study site: Guam

Guam, which is 48 km in length and 6-19 km in width, is both the largest island within Micronesia at an area of 544 square kilometers and the southernmost island of the Mariana archipelago. Northern Guam is

a low-relief limestone plateau (Taborosi et al., 2004) with coastlines characterized by steep cliffs up to about 180 m in height with little to no beach, and to a lesser degree, embayments and stretches of linear beach with fringing reef (Jensen et al., 1997). The terrain of southern Guam consists of mountains, volcanic hills, and isolated regions of karst topography (Mylroie et al., 2001; Taborosi et al., 2004). The highest point on the island is Mount Lamlam at 406 m (Taborosi et al., 2004). Fringing reefs constitute the predominant reef type around the coast of Guam, but other reef varieties include patch, submerged, and barrier reefs (Burdick et al., 2008). The fringing reef platform surrounding the island is typically found at the surface down to a depth of 2 m, and varies in width from tens of meters to several hundred (Burdick et al., 2008). The tides in Guam are mixed semidiurnal with a mean range of 0.5 m and spring tide range of 0.7 m (Pequignet et al., 2011).

The tropical marine climate of Guam is characterized by a dry winter season (December-March) and a wet and humid summer season (June-October). The temperature difference between seasons is approximately 3^o C (Guard et al., 1999). Northeasterly trades prevail during the wintertime, while weaker (roughly 5 kts) and more variable south to southwesterlies constitute the predominant wind pattern during the summertime (Guard et al., 1999). The annual average rainfall in Tiyan (central Guam) is 231 cm (Guard et al., 1999) while the over-water annual rainfall rate is 254 cm (Lander, 2004). July through October are typically the wettest months of the year; however, recorded rainfall on the island can vary substantially on seasonal and annual timescales because strong monsoon surges or tropical cyclones can deliver heavy bouts of rainfall to the island in relatively short bursts. For example, Typhoon Omar brought over 18 inches of rain to Guam in just about a day in August of 1992, and Typhoon Pamela brought 27.01 inches of rain in a 24-hour period in May of 1976 (Guard et al., 1999).

1.4.1 Seasonal monsoon surges

Guam is located in the episodal monsoon regime (Guard et al., 1999). During the summer, sustained periods (at least 3 consecutive days) of strong southwesterly winds generated by monsoon surges can produce significant swell energy, endangering western exposures (Guard et al., 1999). Weak monsoon surges generally produce sustained wind speeds below 13 kts, generate 1-2 m swells, and deliver below 5 cm of rainfall per day to the island (Guard et al., 1999). Strong monsoon surges, which can produce the highest waves that will typically reach the western flank of Guam, bring 10-23 cm of rain per day to the island and are associated with the presence of dense cloud cover, 4-9 m swells, and strong wind gusts up to 50 kts (Guard et al., 1999). These surges can influence the island for a period of two to three weeks at a time (Guard et al.,

1999). A strong monsoon surge accompanied by an intense typhoon can also produce extreme sea levels on western Guam. This scenario occurred in the event of Typhoons Andy (April 1989) and Dale (November 1996) (Guard et al., 1999).

1.4.2 Tropical cyclones

The Western North Pacific (WNP) basin (10^o - 20^oN, 110^o - 160^oE) is characterized by conditions (e.g., weak tropospheric vertical wind shear, strong low-level cyclonic vorticity and upper-level anticyclonic vorticity) favorable for cyclone genesis (Gray, 1968). Guam (as well as the remainder of the WNP) is extremely susceptible to tropical cyclone strikes (Gray, 1968; Guard et al., 1999); the island boasts among the highest rates of typhoon hits within all of Micronesia (Guard et al., 1999). Typhoons in the WNP may form throughout the year, but the months of August through December constitute the most active timeframe for cyclone genesis.

Most tropical cyclones develop within the monsoon trough, a region of low pressure extending from the northwest over eastern Asia (about 20-25^o poleward of the equator) to the southeast of Guam (Lander, 1995; Guard et al., 1999). The east-west axis of the trough delineates a shear zone between low-level (1 km) easterly and southwesterly winds that exist to the north and south of the trough, respectively (Lander, 1994; Lander, 1995). The trough location shifts seasonally and annually in response to fluctuations in sea-surface temperatures and the El Niño Southern Oscillation (Lander, 1995). Occasionally, the monsoon trough reverses its orientation- the trough exhibits a southwest to northeast orientation instead of its average northwest to southeast positioning in the WNP (Lander, 1995). In addition, approximately once per year, the monsoonal circulation in the WNP develops into a large, cyclonic vortex roughly 2000-km wide called a monsoon gyre (Lander, 1994). This mode of the monsoonal circulation is associated with depressed sea-level pressures throughout the tropical WNP (Lander, 1994). Evidently, the monsoon trough is highly migratory in nature.

The surge in water levels produced by tropical cyclones depends primarily on 1) the combined height of the storm tide (storm surge and tidal height) and wave setup, 2) the direction of storm approach, and 3) the characteristics of the nearshore region (e.g., the width and depth of reef) (Guard et al., 1999). The risk of damage posed to coastal communities is greatest in the event of category 3 or higher typhoons, which are associated with stronger winds, heavier waves, and lower atmospheric pressures.

Storm surge, the elevation of water levels due to extreme wind stress and decreased atmospheric pressure, does not necessarily include the influence of tides or setup. The low pressure associated with intense

storms raises sea level by one centimeter for each millibar decrease in pressure through the inverse barometer effect. The decrease in atmospheric pressure alone can produce a surge of 1-1.5 m (Guard et al., 1999). The development of large setup during an extreme high tide will exacerbate already hazardous conditions generated by energetic storm waves and intense winds by allowing waves to propagate farther inland; relatively small storm surges can become hazardous when accompanied by high tides and large setup. The risk of damage to coastal zones is greatest when storm waves approach the shoreline perpendicularly.

A description of the study sites (Apra Harbor, Pago Bay, and Ipan) and the collection of sea-level data from Ipan is provided in Section 2. The wave-driven height contributions to sea level are presented in Section 3, and are compared to tide-gauge records from two additional sites on the island. Origins of some of the prominent sea-level extremes and the influence of tropical cyclones on sea levels around the island are discussed in Section 4.

2 Methods

2.1 Data sources

Historical typhoon tracks from 1945 through 2011 were obtained from the Joint Typhoon Warning Center (JTWC) best track archive via Unisys Weather, a worldwide information technology company. The tropical cyclone coordinates, maximum sustained wind speeds and minimum central pressures were provided in 6-hour intervals for the duration each storm within the archive. The JWTC annual tropical cyclone reports were also used to analyze WNP storm systems.

Atmospheric data (wind speed and gusts, barometric pressure) from Apra Harbor (Station ID: 1630000) and Pago Bay (Station ID: 1631428) during the years 2006-2011 were obtained from the National Oceanic and Atmospheric Association (NOAA). The Apra Harbor measuring station was established in March of 1948, and the Pago Bay station was established in April of 2004. Sea level and atmospheric data are recorded every 6-minutes at the NOAA stations, and are available for download in 6-minute or hourly intervals.

Research-quality hourly sea-level data from Apra Harbor (1948-2011) were obtained from the University of Hawaii Sea Level Center (UHSLC). Hourly tide-gauge observations from Pago Bay (2006-2011) were obtained from NOAA.

2.2 Description of the study sites

2.2.1 Pago Bay

The southeastern coast of Guam is surrounded by fringing reef that spans a width of approximately 120-600 m (Randall and Holloman, 1974). Pago Bay (13.43^{o}N, 144.8^o E) is comprised of a narrow band of rock and coral found on the periphery of the shoreline and a broad reef flat approximately 3 km in length and 750 m at its widest point (Randall and Holloman, 1974). Fine silt and sand of volcanic origin is found solely around the mouth of the Pago River, which drains into the southern portion of the bay, while organic constituents such as foraminiferal remains, shells, and coral debris are more prominent on the reef flat itself (Randall and Holloman, 1974). The reef margin is characterized by spur and groove topography. The mean tidal range in Pago Bay is 0.34 m and the diurnal range is 0.49 m (NOAA); the shallowest portions of Pago Bay are aerially exposed during low tides. The University of Guam Marine Laboratory is situated on the northeastern portion of the bay.

2.2.2 Apra Harbor

Apra Harbor (13.43^{o}N, 144.65^{o}E), serving dually as a naval base and commercial port on western Guam, consists of an inner section that extends southward from the eastern portion of the outer harbor. Cabras Island and a partially man-made breakwater called Glass Breakwater delineate the northern periphery of the outer harbor while Orote Peninsula forms the southern boundary of outer Apra Harbor. The harbor waters are comprised of patch, fringing, and barrier reefs (Burdick et al., 2008). In some areas, the water depth exceeds 30 m (Gilmore et al., 1995). The mean tidal range in Apra Harbor is 0.49 m and the diurnal range is 0.71 m (NOAA).

2.2.3 Ipan

Ipan (13.35^{o}N, 144.78^{o}E) is located on the southeastern coast of Guam in the village of Talofofo. The reef flat, a smooth, 450-m wide stretch of carbonate pavement covered by macroalgae, extends from the shoreline of a narrow beach to the reef margin; there is a sharp transition between the reef flat and fore reef (Pequignet et al., 2011; Vetter et al., 2010). The fore reef, characterized by rough spur and groove topography with vertical coral walls and scattered boulders, consists of a relatively steep face that stretches for about 5 m and then gently deepens at a 4^o slope thereafter (Pequignet et al., 2011; Vetter, 2007). The average water depth over the reef platform is 0.5 m, but the reef flat is exposed during extreme low tides (Pequignet et al., 2011). Figure 2 shows the locations of Apra Harbor, Ipan, and Pago Bay.

2.2.4 Wave attenuation at the Ipan reef

Coastal features influence the transfer of wave energy from the open ocean to the shoreline via shoaling, refraction, and wave breaking. Due to the high bottom roughness of reef environments relative to sandy beaches, reefs can protect coastal areas during large wave events through attenuation of incoming wave energy (Roberts et al., 1977; Lugo-Fernandez et al., 1998). During small wave conditions, the high bottom friction associated with coralline areas accounts for most of the dissipated wave energy; however, during large wave conditions, breaking becomes the dominant wave-dissipation mechanism (Lowe, 2005). At the Ipan reef, about 80% of energy dissipation (for waves in the incident swell band) is attributed to wave breaking, while the remainder is linked to bottom friction on the fore reef (roughness coefficient of 0.2), and to a much lesser extent, the reef flat (roughness coefficient of 0.06) (Pequignet et al., 2011). Incident swell wave heights show a 97% decrease over all water depths (low and high tides) along the reef. Significant wave heights from the fore reef to the reef crest decrease by an order of magnitude (Pequignet et al., 2011; also, see Figure 3).

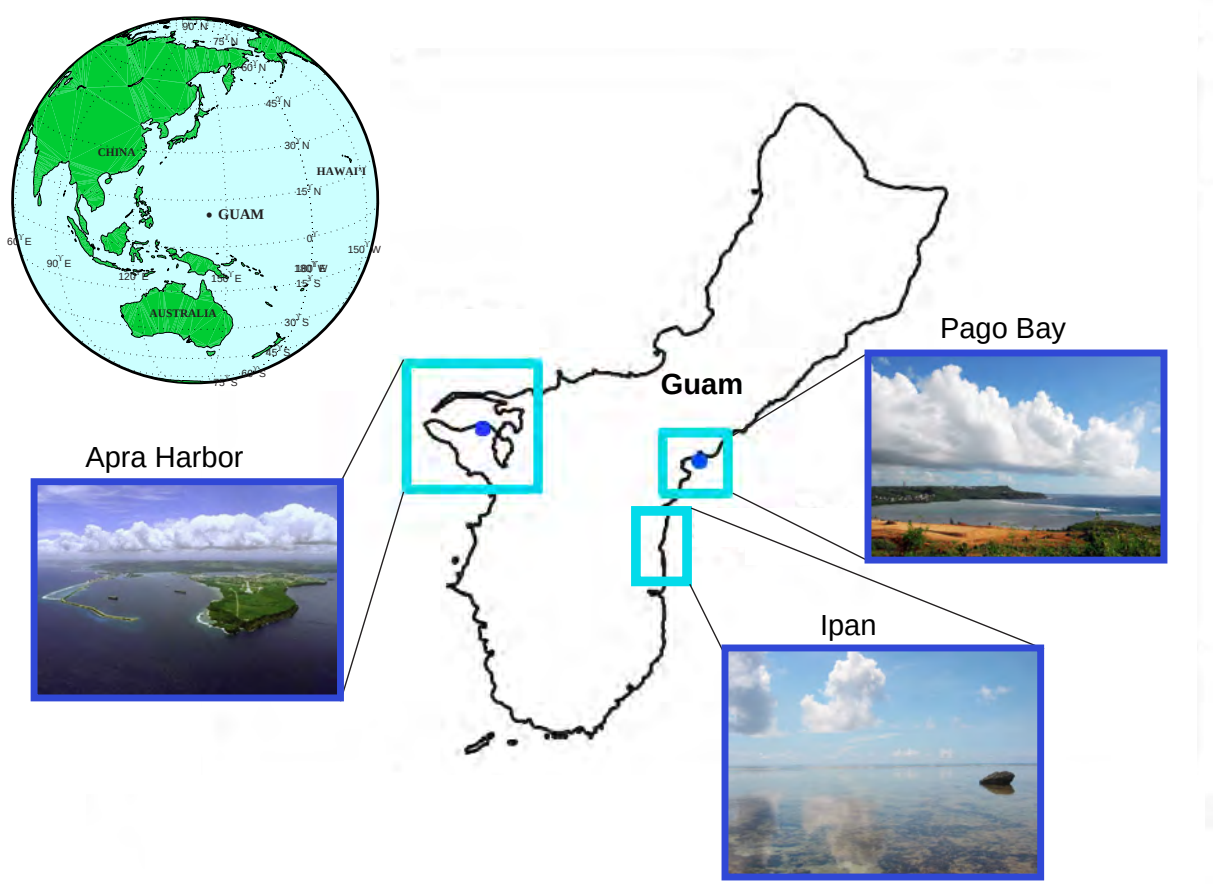

Figure 2: Map of Guam. The locations of Apra Harbor, Ipan, and Pago Bay are boxed. The solid blue points denote the location of the NOAA tide gauges utilized here. The location of Guam on a globe is shown in the top left-hand corner.

In reef environments where the breaker zone is limited to a wide and shallow reef flat, transmission of incident swell energy into the reef zone is largely depth limited, i.e., dependent on the water level above the reef (Pequignet et al., 2011). During a heavy swell event, wave heights on the reef flat increase as a result of the water-level elevation over the flats in the form of setup. High tides may also produce a similar effect on wave heights by increasing the water depth over the reef flat, but at Ipan, when the waves exceed 2 m, setup heights exceed the tidal range (Pequignet et al., 2011).

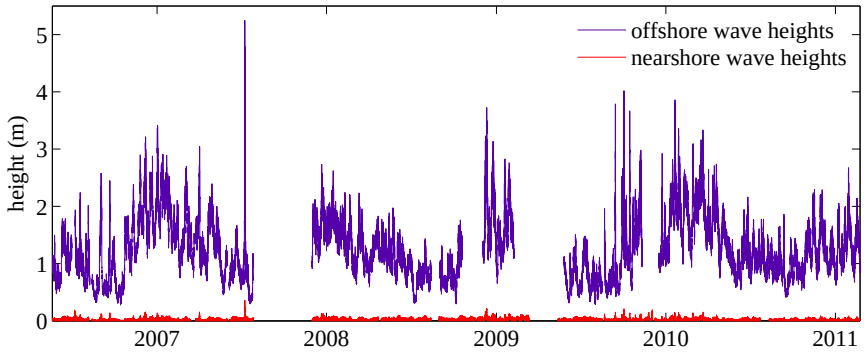

Figure 3: Attenuation of wave heights from the fore reef to the reef flat.

2.3 Collection of data at Ipan

A cross-shore array of instruments (Seabird 26plus pressure sensors and Nortek Aquadopp current profilers) was deployed across the Ipan reef platform and the fore reef for varying durations of 3 to 6 months for a 5-year period from August 2005 to February 2011 as part of the Pacific Island Land-Ocean Typhoon (PILOT) project (Pequignet et al., 2011). All instruments sampled at a frequency of 1 Hz. Figure 4 shows the location of all the instruments; the sensors marked in blue (2 and 10) were used in this study. Data obtained during extreme low tides, in which the reef flat sensors were aerially exposed, were not used in the analysis.

2.4 Computation of setup and extreme runup

The data was initially preprocessed- linear trends were removed from the sea-level records in order to account for sensor-related pressure drifts (Pequignet et al., 2011). Fifteen-minute sea level averages were computed using the 1-Hz data. Following Vetter et al. (2010) and Pequignet et al. (2011), wave setup on the reef flat was estimated by computing the difference between the averaged water levels from sensors 2

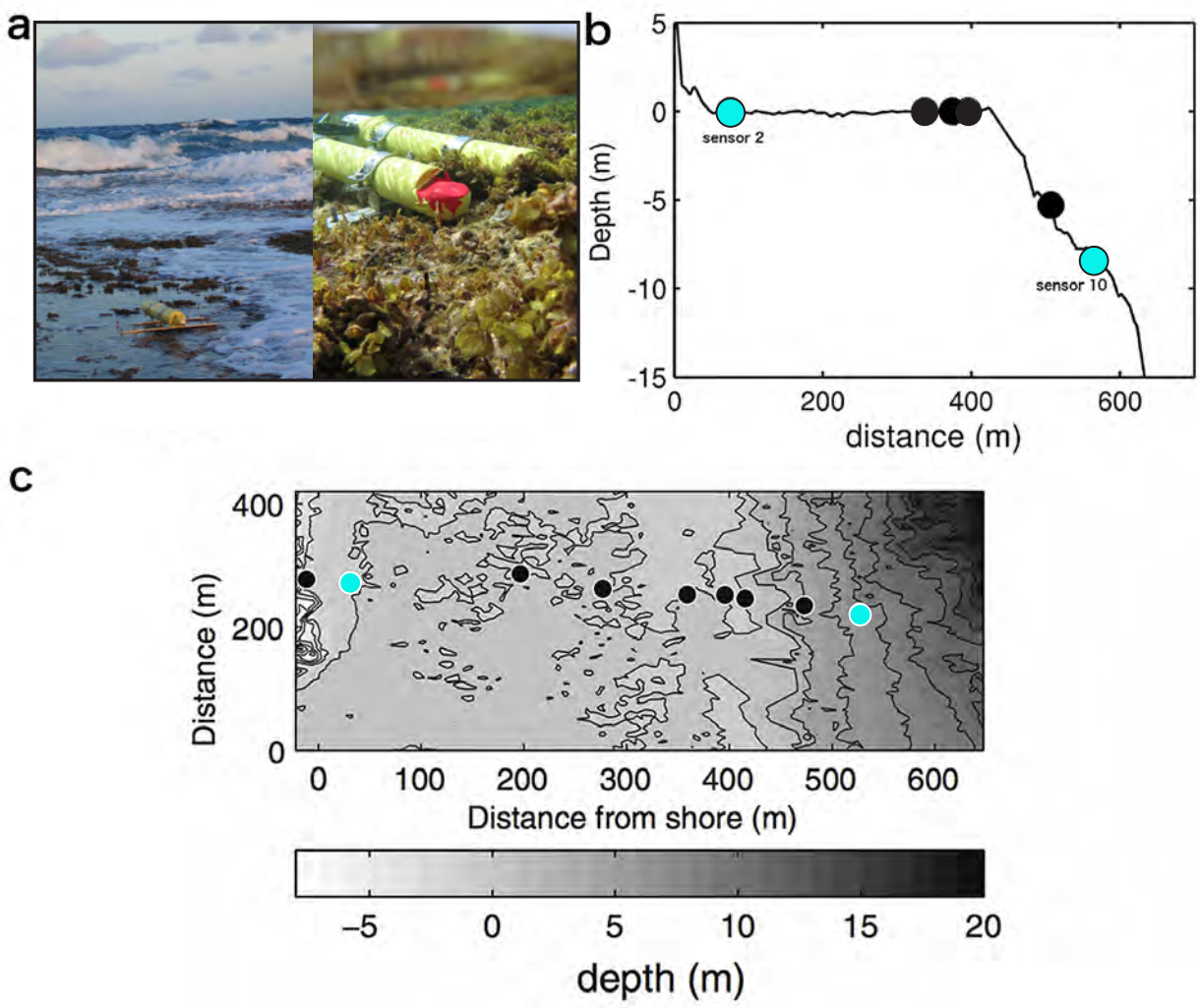

Figure 4: Ipan study site. **a** Location of the Ipan reef, **b** Depth of each of the instruments as a function of its distance from the shoreline. **c** Bathymetry of the Ipan reef from SHOALS data with the locations of the sensors marked (those used in this study are delineated by blue circles).

and 10. Sensor 10 effectively measures sea level and tidal effects (and some wave setdown), while sensor 2 effectively measures the sea level, tidal effects, and wave setup; thus, the difference between the two sensor observations yields an estimate of setup on the reef. An offset term was specified such that wave setup is zero when incident wave heights at sensor 10 are zero (setup heights should be zero when there are no waves). It was assumed that the setdown at sensor 10 is negligible; Vetter et al. (2010) found a difference of roughly 7% in the observations when setup was referenced to wave heights at sensor 10 including the effects of setdown.

The influence of the tides and setup were removed from the unaveraged 1-Hz data for each deployment by detrending the sea-level observations from sensor 2. This data was reshaped into 15-minute subsets, and each subset was subsequently sorted according to height. Extreme runup, defined here as water levels exceeding the 98-percentile threshold, was computed as the mean of the top 2% of the detrended sea levels. The combined setup and extreme runup contributions, added to the baseline water level measured by sensor 10 (depth of this sensor was accounted for), yielded water levels at Ipan with wave effects on sea level included into the observations.

3 Results

Figure 5 shows sea-level data (offshore wave height, wave setup, nearshore sea level) and meteorological observations (wind speed and atmospheric pressure) from the study period (May 2006 through February 2011); Table 1 shows statistics (mean, median, mode, min, and max values) associated with the oceanic and atmospheric data. The peak wave height (5.2 m), sea level (0.36 m), and wind speed (28 kts) at the Ipan reef were recorded from 9-10 July 2007 as tropical depression Man-Yi (which later strengthened into a typhoon) passed to the south of Guam (see section 4.2). The waves generated by Man-Yi produced setup maxing out at 1.3 m (see Figure 5).

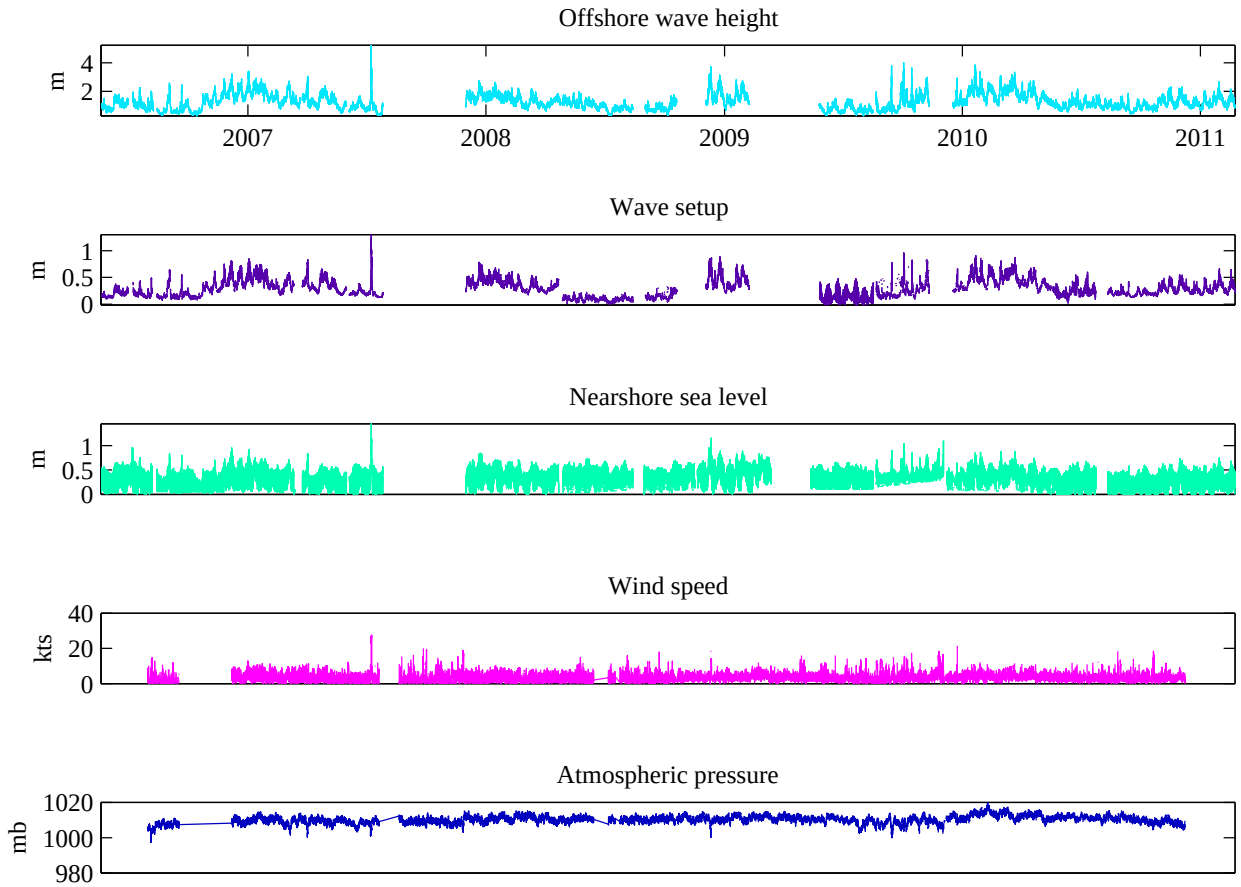

Figure 5: Ocean and atmosphere conditions during the study period (2006 - 2011). The sea-level observations were obtained from the pressure sensors at Ipan, while the wind and pressure data were obtained from NOAA. See also Table 1.

.

The Ipan water levels including the additional height elevation produced by setup and runup were compared to the Apra Harbor and Pago Bay tidal data (see Figures 6, 7). Figure 6 shows the complete sea

level record from Apra Harbor (1948-2012) compared to computed water level including wave effects at Ipan during the 5-year study period (2006-2011). The difference between the tide-gauge measurements and the sea level including wave influences on water levels is quite significant- wave-driven setup and runup produced a mean sea surface height elevation of 0.3 m during the deployment period and a maximum elevation of 1.5 m during the passage of tropical depression Man-Yi in 2007. While sea levels from Apra Harbor were used in this analysis because they constitute the longest sea-level observations from the island, it is important to note that the difference between the Ipan and Apra Harbor water levels could be somewhat exaggerated since southeastern exposures tend to be more susceptible to swell activity than the western coast of the island (Guard et al., 1999).

Table 1: Statistics associated with oceanic and atmospheric conditions for the deployment period. H_2 and H_{10} represent the wave heights at sensor 2 and sensor 10, respectively. The dates in which the maxima and minima for the parameters occurred are denoted in parentheses.

	H_{10} (m)	Setup (m)	H_2 (m)	Wind speed (kts)	Pressure (mb)
Mean	1.16	0.261	0.0240	3.62	1010
Median	1.07	0.233	0.0194	3.31	1010
Mode	0.278	-0.0143	0	3.11	1010
Max	5.24 (7/9/07)	1.3 (7/9/07)	0.357 (7/9/07)	27.6 (7/10/07)	997 (8/5/06)
Min	0.2783 (10/14/06)	-0.0143 (7/21/09)	0 (9/16/08)	0 (12/9/10)	1019 (2/9/10)

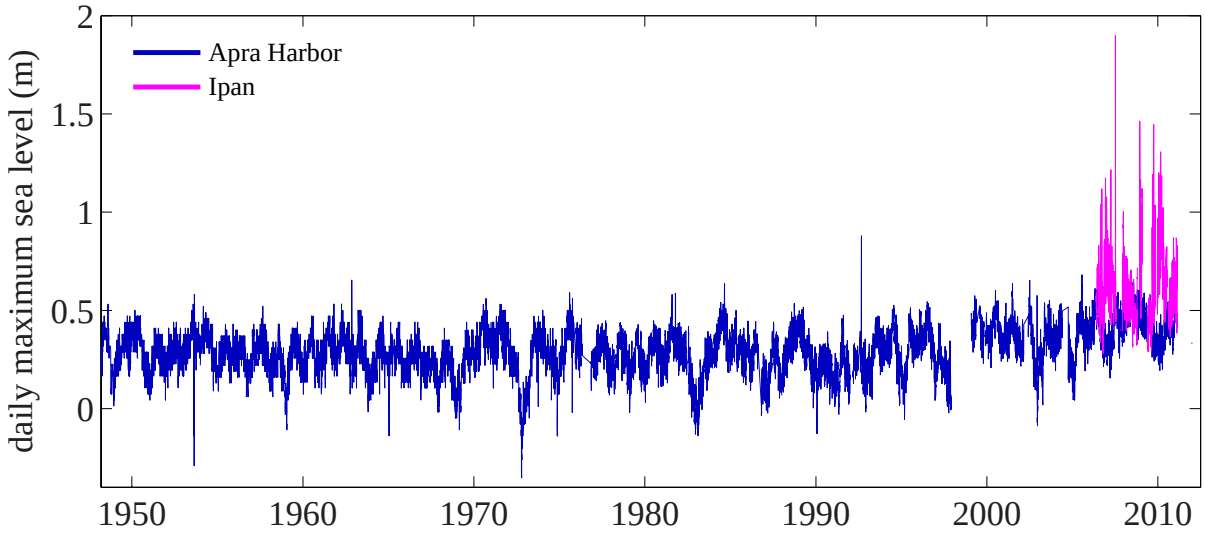

Figure 6: Daily maximum sea level at Ipan and Apra Harbor. Shown in blue is the daily maximum sea level using the tide gauge data at Apra Harbor from 1948 to present, and shown in magenta is sea level in Ipan including wave-driven effects from 2006-2011.

Figure 7 shows the daily maximum water levels from Ipan (with and without wave effects), Apra Harbor, and Pago Bay. Periods in which the daily maximum sea levels at Ipan closely match the Apra Harbor tide-gauge record are observed in the data; examples include sea-level observations from mid-2008 and 2009 (see Figure 7). These were periods characterized by small wave conditions (⁄2 m), as shown in the offshore wave height timeseries in Figure 5 (top panel), and therefore small coastal setup.

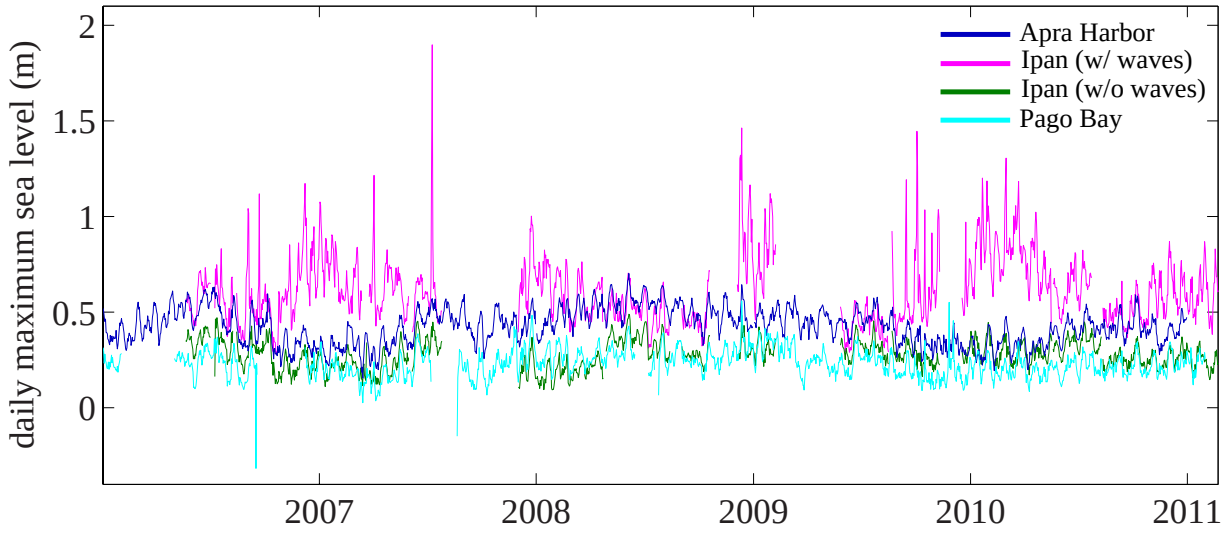

Figure 7: Daily maximum sea level in Apra Harbor, Ipan, and Pago Bay from 2006-2011.

The disparity between the water level with and without wave effects included into the sea-level record is especially pronounced when the wave heights at the fore reef exceed 2 m. For example, the most significant difference between the computed sea level (with wave effects) and the tide-gauge records is observed during the passage of Man-Yi in July of 2007 (see Figures 5, 6, 7). The disparity between the water level with and without wave-driven effects may be even more drastic if a large, intense tropical cyclone passed directly or almost directly over Guam at a very slow translational speed (therefore allowing waves to intensify because of the longer fetch length and duration); however, no such storms occurred from 2006 to 2011.

4 Discussion

4.1 Tropical cyclone tracks

Using JWTC best-track storm data from 1945-2011, it was found that most of the 273 tropical cyclones (43%) that came within 290 km (155 nm) of Guam (13.45^{o}N, 144.78334^{o}E) with maximum sustained winds of at least 45 knots approached the island from the southeast (Figure 8a). A considerable percentage of storms (37%) also approached the island from the northeast, but relatively few tropical cyclones approached Guam from either the northwest (5%) or southwest (15%). These storm headings were obtained through a visual inspection of the storm tracks corresponding to all of the cyclones meeting the aforementioned distance and wind requirements. The storm heading was determined at the point of closest approach to Guam, a process that required subjectivity because the coordinates of the storms were available only on 6-hour intervals from the JWTC archive. The tracks associated with all of the storms analyzed here are shown in Figure 8b.

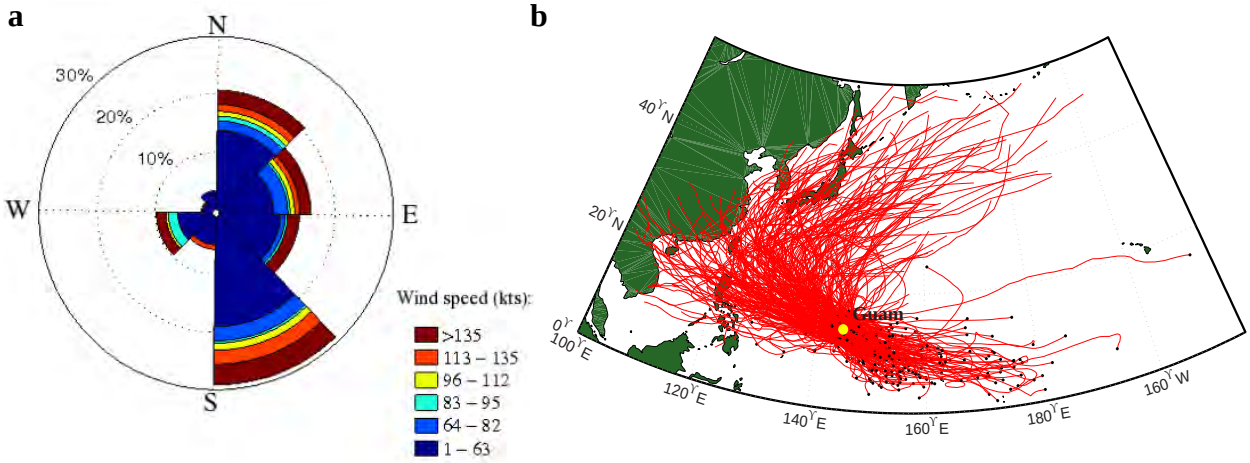

Figure 8: Typhoons affecting Guam from 1945-2011. **a** Direction of storm approach for tropical cyclones with maximum sustained winds of at least 45 knots coming within 290-km of Guam. Storm headings were determined at the point of closest approach using data from the JWTC best-track archive. **b** Tracks of the storms represented in **a**. Most storms approach Guam from the southeast and veer toward the northwest after passing the island.

According to Guard et al. (1999), extreme sea levels are more frequent on the eastern exposures of Guam due to the favored east-to-west track of tropical storms in the WNP (Guard et al., 1999). Guard et al. (1999) found that historically, up to 85% of tropical cyclones that came within 330 km (180 nm) of Guam displayed a westward component to their motion. In this study, it was found that roughly 80% of the storms (that satisfied the wind and distance requirements set here) approached Guam from the east and then passed to the west of the island. Gilmore et al. (1995) found that most storms approach the island from the

east-southeast and then veer toward the west-northwest after passing Guam. Due to this preferred cyclone track, the eastern and southeastern shores of Guam remain the most vulnerable (and western exposures the least vulnerable) to inundation from storm surge and setup produced by tropical systems (Guard et al., 1999; Gilmore et al., 1995).

4.2 Sea-level response to typhoons in Guam

Typhoons Man-Yi (7-15 July 2007) and Dolphin (8-18 Dec 2008) passed 385 km (207 nm) and 75 km (40 nm) to the south of Guam, respectively, during the study period (see Figure 9 for their storm tracks). Man-Yi traveled past Guam as a tropical depression with maximum sustained winds of 30 knots (wind gusts of up to 40 knots were recorded at Pago Bay, see Table 2) and a minimum central pressure of 1000 mb. The storm produced offshore wave heights from the southeast maxing out at 7 m and a period of 11 s (Pequignet et al., 2011). Sea level at Apra Harbor peaked at 0.57 m during the passage of this tropical depression; unfortunately, sea-level observations from Pago Bay were not available from 8 July through 19 August 2007. At the Ipan reef, sea level with setup and extreme runup included into the observations was about 1.3 m on 8 July and nearly 2 m on 9 July (see Figure 10). A disparity of approximately 1.5 m was observed between sea level with and without wave-driven effects during the passage of this storm (Figure 10). Man-Yi later strengthened into a category-4 typhoon with maximum sustained winds of about 125 knots and a minimum central pressure of 929 mb. Although Guard et al. (1999) found that storms that come within 330 km of Guam produce "some effect" on the island (and storms that come within roughly 135 km of the island are expected to have a more direct effect on Guam), it is found here that storms as far as 385 km (200 nm) from the island can have a pronounced effect on sea levels in Guam, as in the case of Typhoon Man-Yi.

Dolphin passed to the south of Guam as a tropical depression with maximum sustained winds of about 30 knots and a minimum central pressure of 1000 mb. Maximum wind gusts up to 32 kts were observed at Apra Harbor, while wind gusts up to 22 kts were recorded at Pago Bay (see Table 2). Sea level at Apra Harbor and Pago Bay peaked at 0.56 and 0.64 m, respectively, on 11 Dec 2008 in response to the passage of Dolphin. On the same day, the computed water level with wave effects included into the observations was approximately 1.5 m in Ipan (Figure 10). A disparity of about a meter between water levels with and without wave effects was observed as Dolphin traveled past Guam (Figure 10). This storm later strengthened into a category-2 typhoon with maximum sustained winds of 90 knots and a minimum central pressure of 955 mb (JWTC).

Atmospheric data associated with Typhoons Dale (4-13 Nov 1996), Paka (28 Nov - 22 Dec 1997), Pongsona (1-10 Dec 2002), all of which caused extensive levels of damage across the island, are also included here because these storms constitute the most intense typhoons to affect Guam in recent times (see Table 2 for data). Sea-level observations from December of 1997, corresponding to the passage of Typhoon Paka over the island, are not available. Typhoon Dale, which caused an estimated $3.5 million of damage on Guam, passed 205 km (110 nm) to the south of the island with maximum sustained winds of 90 knots on 7 Nov 1996. The island was exposed to the peripheral rain bands of Dale, but not the eye-wall cloud (Dillon and Andrews, 1996). The passage of Dale led to widespread inundation of low-lying coastal zones and erosion of numerous beaches on western Guam. The western shorelines of the island were reportedly subjected to "phenomenal seas" of 6-9 m (20-30 ft) following the passage of Typhoon Dale, with runup heights peaking at an estimated 30 m at Orote Point (Dillon and Andrews, 1996). On 9 Nov, after Dale had moved west of Guam, the storm attained super-typhoon status (Dillon and Andrews, 1996).

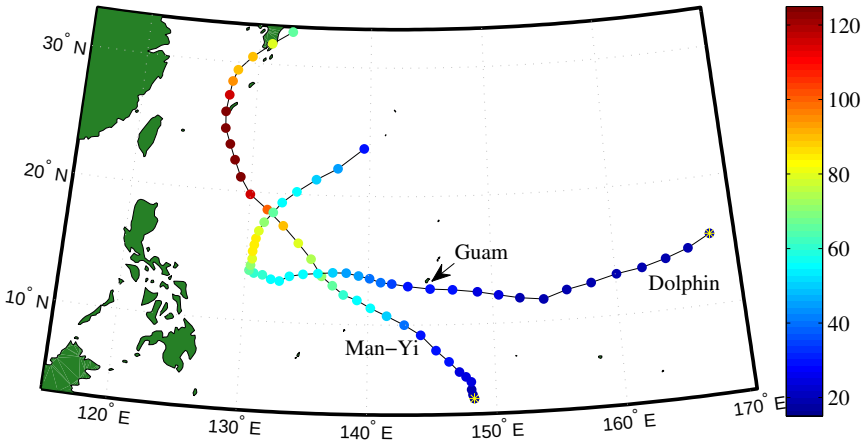

Figure 9: Storm tracks of Typhoons Man-Yi (July 2007) and Dolphin (Dec 2008). The yellow asterisks denote the origin of the storms. The markers are filled in with the maximum sustained wind speeds of the storm (obtained from the JWTC best-track archive).

Typhoon Paka, with sustained surface winds of 130 kt gusting to 160 kt, passed over northern Guam on 16 Dec 1997. A minimum pressure of 957.6 mb and a maximum wind gust of 97 kts was recorded at Apra Harbor on 16 Dec (Table 2). Paka caused severe damage in northern parts of Guam, but about 20 km to the south of where the eye wall cloud passed, minimal losses were reported (Dillon and Andrews, 1997). Typhoon Pongsona passed very close to Guam as a category-4 typhoon with maximum sustained winds of 130 knots and a minimum central pressure of 910 mb. Over 200 individuals were injured and 3 were killed in the wake of Typhoon Pongsona. Substantial damage to the power, sewage, and water systems and coastal

infrastructure was incurred; nearly 2,000 individuals were left homeless (Furze and Engel, 2002).

Interestingly, a marked increase in sea levels at Apra Harbor was not observed during the passage of Typhoons Dale and Pongsona (Figure 10) even though these storms constitute among the most severe tropical systems to strike Guam (Dillon and Andrews, 1996; Furze and Engel, 2002). Water levels from neither Pago Bay nor Ipan were available during the passage of these two typhoons over the island, but it would have been of interest to see how sea levels with setup and runup included into the observations would compare to Apra Harbor tidal levels at these times.

Table 2: Oceanic and Atmospheric Data from Apra Harbor and Pago Bay for major storms occurring from 1996 - present. Values in parentheses were obtained from the Pago Bay station.

	Dale (Nov 96)	Paka (Dec 97)	Pongsona (Dec 02)	Man-Yi (Jul 07)	Dolphin (Dec 08)
Min pressure	989.7	957.6	992.8	1002 (1001)	1000 (1001)
Max wind speed	38.9	97.0	36.5	27.2 (27.6)	20.8 (18.3)
Max wind gust	60.8	70.8	51.5	- (38.9)	32.2 (22.9)

The tracks of the most significant cyclones to affect Guam since 1945 are shown in Figure 11a, and data associated with these storms (e.g., maximum sustained winds, direction of approach, translational velocity) can be found in Table 3. This compilation of historically significant typhoons was produced by updating a list of particularly severe tropical cyclones retrieved from the Guam Typhoon Vulnerability Report (Guard et al., 1999). Typhoons Dale and Pongsona are included in this collection of major typhoons. The maximum recorded sea levels during the passage of each of these storms were identified in the Apra Harbor tide-gauge observations (see Figure 11b). Analysis of these sea-level maxes shows that water level at Apra Harbor does not deviate significantly from mean levels during the passage of intense typhoons (category 3 or higher) directly or almost directly over the island.

4.3 Sea-level extremes at Apra Harbor

In order to identify extreme sea levels generated principally by large storm surges as opposed to extremes produced by moderate surges and extreme tides, for example, various signals were eliminated from the Apra Harbor tide-gauge record. ENSO in particular is known to have a relatively significant effect on sea levels in the Western North Pacific- ENSO influences water levels in Guam directly (via the rise and fall of sea levels in response to changes in wind patterns associated with ENSO) or indirectly (via shifts in the location of cyclone genesis). During El Niño years, mean sea levels fall in Guam as well as the remainder of Micronesia; water levels typically reach a minimum in December of an El Niño year and rise to average values by spring of the following year. The risk of a typhoon strike on Guam increases from 1 in 10 to 1 in 3 during

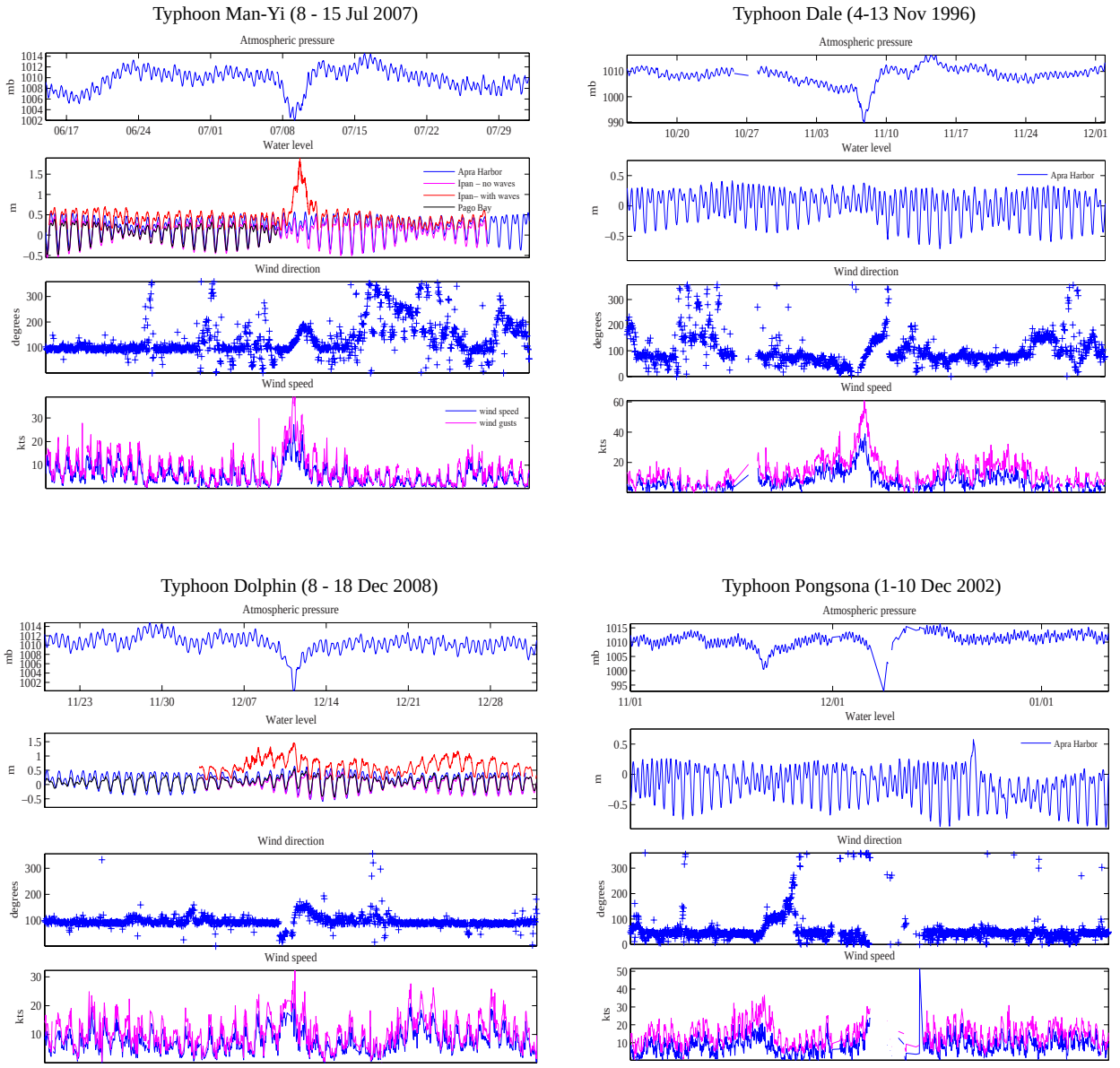

Figure 10: Atmospheric and oceanic data for Typhoons Man-Yi, Dolphin, Dale, and Pongsona. Sea-level data from Apra Harbor, Ipan, and Pago Bay were available for Typhoons Man-Yi and Dolphin; water levels with and without wave effects are shown in the sea-level panels. Only tidal data from Apra Harbor was available during Typhoons Dale and Pongsona.

Table 3: Summary of major storms affecting Guam from 1945 to the present. Table includes the name of the storm, its minimum distance from Guam, the maximum wind speed provided by the JWTC best-track archive, its direction of approach (determined at the point of closest approach to Guam), and its average velocity. The average velocity of the typhoons were calculated when the storms were within 375 km of the island using data from the best-track archive.

Storm dates	Name	Min dist (km)	Max winds (kts)	Dir. of approach	Average velocity (km/hr)
10 - 24 Aug 1951	Marge	55	70	SE	18
7 - 18 Nov 1962	Karen	17	150	SE	32
14 - 29 May 1976	Pamela	21	120	SE	14
6 - 17 Nov 1977	Kim	25	65	NE	30
1 - 9 Oct 1982	Mac	50	70	SE	14
8 - 22 Nov 1984	Bill	74	85	SE	32
16 Nov - 1 Dec 1991	Yuri	100	150	SE	32
20 Aug - 6 Sep 1992	Omar	direct hit	115	SE	14
13 Nov - 1 Dec 1992	Gay	direct hit	95	SE	25
4-13 Nov 1996	Dale	205	90	SE	30
28 Nov - 22 Dec 1997	Paka	direct hit	135	NE	14
1-10 Dec 2002	Pongsona	direct hit	130	SE	18

El Niño years because the eastward shift of the monsoon trough allows storms to travel and intensify over longer stretches of warm water (Guard et al. 1999; Lander, 2004). During La Niña, sea levels throughout the WNP are elevated above average values, and the monsoon trough shifts westward of its annual average position (Lander, 2004). The chances of a typhoon strike on Guam and most of Micronesia decrease during this phase of ENSO.

The annual mean sea level and the tidal, ENSO, semi-annual and annual signals were eliminated from the Apra Harbor observations to isolate the surge component of water levels; actual surge heights are expected to be larger than those recorded at Apra Harbor, however, because the tidal measurements do not likely account for wind-driven wave activity during storms. The maximum water levels corresponding to the passage of each of the major typhoons (Table 3) were again identified within this modified sea-level record. The results of this analysis are shown in Figure 11c.

The reason(s) the majority of severe tropical cyclones listed in Table 3 did not produce a more significant effect on Apra Harbor sea levels is not fully understood. While it was not anticipated that observations from the harbor would be influenced significantly by wind-driven waves produced by the tropical systems, a more prominent sea-level response to depressed atmosphere pressures via the inverse barometer effect was expected.

The peak-over-threshold method, with the threshold set at 98-percentile level, was used to find extreme sea levels within the record (the extremes are delineated by purple markers above the dashed line in Figure 11c). The sea levels recorded during the passage of Typhoons Marge and Omar exceed the 98-percentile

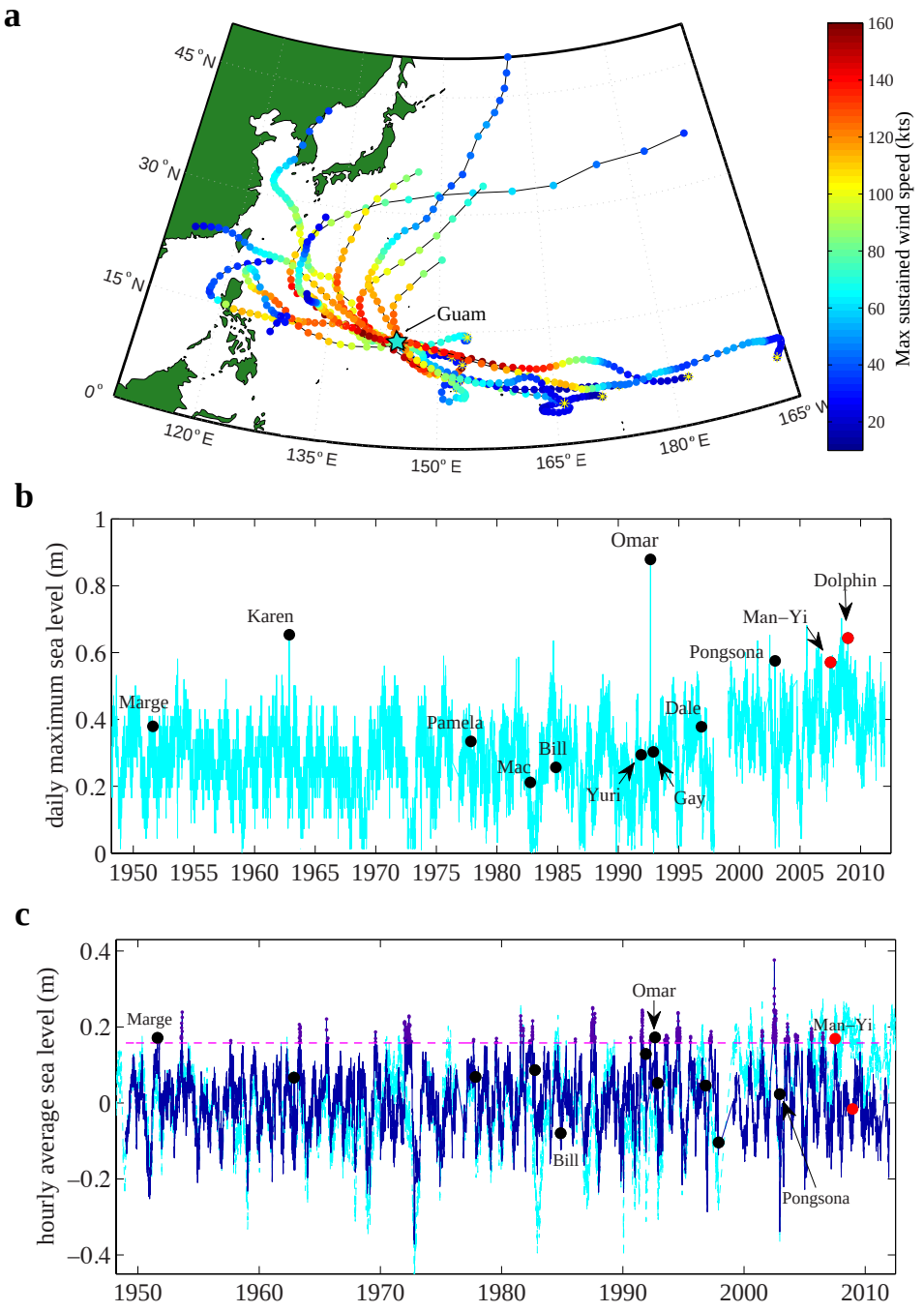

Figure 11: **a** Tracks of the most severe typhoons to influence Guam. The yellow asterisks denote the origin of each of the tropical cyclones. These storms are listed in Table 3. **b** Daily maximum sea level from Apra Harbor. Water levels corresponding to the passage of the typhoons from **a** are delineated by black markers. **c** Daily sea-level from Apra Harbor with the annual average sea level removed. Tidal, ENSO, semi-annual, and annual signals were also eliminated from the record. Sea levels corresponding to the passage of the typhoons in **a** are represented by black markers. Small purple markers shown above the magenta dashed line denote sea levels exceeding the 98-percentile threshold.

threshold set in this study (Figure 11c); water levels corresponding to the passage of Typhoon Man-Yi also exceed the threshold set here even though this storm was not as intense (lower sustained wind speed and higher central pressure) as the storms listed in Table 3 and did not pass as close to the island as these other, more severe storms. According to the 1997 annual tropical cyclone report, Typhoon Karen (135 kt winds gusting to 165 kt) was more intense than both Pamela (May 1976) and Omar (August 1992), but the sea-level response to the passage of Omar over northern Guam is the most significant in the Apra Harbor tide-gauge record. Evidently, fluctuations in the surge component of sea level at Apra Harbor do not necessarily depend on cyclone intensity or proximity to Guam (see Figure 11c, also 12).

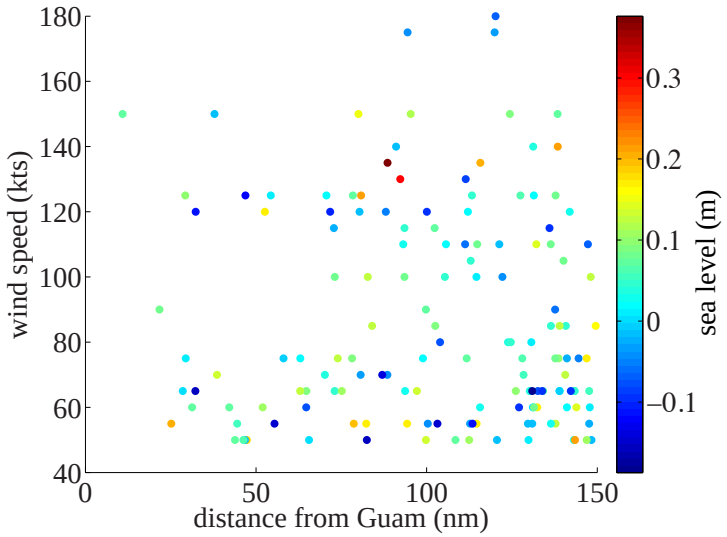

Figure 12: Winds versus distance scatterplot filled in with the surge component of sea level from Apra Harbor. No correlation between sea level and storm intensity/proximity is observed.

Some of the prominent peaks in the Apra record vanish when the surge component is separated from the other sea-level constituents. For example, the pronounced peak in water levels corresponding to the passage of Typhoon Omar in August of 1992 disappears when the annual average sea-level and the tidal, ENSO, semi-annual, and annual signals are removed from the observations (see Figures 11b and c). The estimated path of the eye of Typhoon Omar passed over the Naval Air Station on 28 Aug 1992 (Mautner and Guard, 1992). Omar intensified rapidly before striking Guam with 105-kt sustained winds, causing an estimated $457 million worth of damage (Mautner and Guard, 1992). According to the Annual Tropical Cyclone Report (Dillon and Andrews, 1996) report, the storm surge associated with the passage of Typhoon Omar fell short of predictions, but the arrival of the storm coincided with an extreme high tide; this observation

may account for the spike in sea level observed in Figure 11b. Interestingly, Typhoon Man-Yi produced approximately the same level of surge as Typhoon Omar, which hit Guam directly and was characterized by higher sustained winds and a lower minimum central pressure (see Figure 11c).

4.4 Causes of extreme sea levels

Table 4 shows some of the most prominent sea-level extremes observed at the harbor as well as the event(s) or condition(s) that may have produced the high waters (if a cause could be identified). At least 5 days between each extreme was required in order for it to be considered as a separate high-water event. The JWTC best-track data and annual tropical cyclone reports were searched to identify the origins of the extremes at Apra Harbor, but this process was difficult and marked by uncertainty. Many of the extreme high waters at the harbor could not be linked to a particular event. Some of the sea-level extremes were attributed to typhoons that passed to the west of Guam; however, the recorded high waters may not actually be related to the cyclones that were identified. For example, the tropical cyclone may have been near Guam (< 330 km) at the time an extreme was recorded at Apra Harbor even though the high waters were produced by another tropical disturbance, strong monsoonal gales, or some other system nearby.

Table 4: Extreme sea-level events at Apra Harbor (1949-2011).

Event date(s)	Sea level (m)	Cause
17 Jul 1987	0.200877	
28 Apr 1972	0.201579	
4 Jun 1972	0.205295	
6 Jun 2002	0.205712	
29 Apr 1963	0.206825	Typhoon 1 (27 Apr - 6 May)
2 Aug 2003	0.208396	
10 Aug 1953	0.210073	Super typhoon 8 (8-18 Aug)
21 Jun 2002	0.211712	
23 Jun 1987	0.213200	
2 Jan 1972	0.213389	
10 Jul 2002	0.214278	Super typhoon 10 (5-16 Jul)
23 Jul 1982	0.216183	Typhoon 10 (21-30 Jul)
15 Jul 1987	0.217280	Typhoon 6 (15-22 Jul)
22 Jul 1965	0.221057	Typhoon 14 (21-27 Jul)
10 May 1972	0.228231	
1 Aug 1981	0.229150	
4 Sep 1987	0.235529	
25 Jul 1994	0.237133	southwesterly monsoon winds
27 Aug 1953	0.239084	
14 Aug 2002	0.242333	
30 Jun 2002	0.2427117	
13 Aug 1991	0.244213	southwesterly monsoon winds
8 Jul 1987	0.250690	
4 Jul 2002	0.376236	

The extreme sea levels listed in Table 4 appear to be highly concentrated in the months of June, July, and August, and only a few of these extremes occurred before 1980. One of the highest extreme events recorded at Apra Harbor, namely the August 1991 event, may have been related to the formation of a monsoon gyre in early August of 1991. The monsoon gyre persisted in the WNP for nearly a month (Rudolph and Guard, 1991). This gyre migrated in a west-southwesterly fashion from its location of genesis (west of Guam) and passed north of the island, bringing monsoon southwesterlies to the island for roughly two weeks (Lander, 1994).

It is likely that a particular combination of oceanic and atmospheric conditions is required for a pronounced sea-level increase to be observed within the harbor during the passage of a typhoon. A storm passing directly south of Guam (as opposed to directly north) exposes the island to the dangerous semicircle, the region within the tropical cyclone characterized by stronger winds and heavier seas (Guard et al., 1999). The rotational and translational wind-field components become additive on the right (left) side of the storm with respect to the direction of cyclone movement in the Northern (Southern) Hemisphere, causing the wind speed and wave-height distribution within the moving storm to display asymmetry in intensity. Thus, a storm passing to the south of Guam has more destructive potential than a storm passing to the north of the island. For example, Typhoon Yuri passed 100 km south of Guam (exposing the island to the "dangerous semicircle") in November of 1991 as a category-5 super typhoon with maximum sustained winds of 150 knots and a minimum central pressure of 885 mb. This storm generated estimated runup heights of 7.5-9 m (25-30 ft) on exposed areas of southeastern Guam, causing heavy flooding, beach erosion, and reef damage (Rudolph and Guard, 1991).

Extreme sea-level events on western Guam may occur when a storm approaches the island from the south-southwest and advances nearly parallel to the western coastline in a north-northwesterly fashion, but such a scenario is not observed frequently because of the favored east-to-west cyclone track in the WNP (Guard et al., 1999). According to Guard et al. (1999), a more probable storm-event scenario involves a large, intense (at least category 3), and slow-moving typhoon passing directly south of Guam. This combination of storm features was observed in the wake of Typhoon Karen in November of 1962, Pamela in May of 1976, and Omar in August of 1992 (Guard et al., 1999). The sheer size of the storm exposes western Guam to the strong winds and seas associated with the eyewall, and the slow translational velocity of the storm allows for the development of heavier swells due to increased fetch length and duration. However, as shown in this study, only Typhoon Omar produced water levels at Apra Harbor exceeding the 98-percentile threshold.

4.5 Storm intensity and swell size

In addition to the absence of a correlation between sea level and storm intensity/proximity, there does not appear to be a well-defined correlation between cyclone intensity and swell size (Dillon and Andrews, 1996). For example, Typhoon Omar passed directly over the island as a category-3 typhoon with 105 knot winds and a pressure of 940 mb in August of 1992 (Dillon and Andrews, 1996). However, Omar failed to produce swells comparable to the 6-9 m (20-30 ft) seas that were observed in western Guam in response to the passage of Typhoon Dale, which passed about 200 km (110 nm) south of the island with a maximum sustained wind speed of 90 knots (Dillon and Andrews, 1996).

The height of the swell generated on western Guam appears to depend on a multitude of factors. In particular, heavy westerly swells may be produced when the passage of an intense typhoon over the island is accompanied by gale-force (>33 knots) monsoonal southwesterlies (Dillon and Andrews, 1996; Guard et al., 1999). This scenario is exemplified by Typhoon Dale (see previous section) and Typhoon Andy, which occurred in April of 1989 and passed 130 km (70 nm) southeast of Guam as a super typhoon with 135-140 kt winds. Interestingly, the passage of these storms across the island do not constitute extreme events within the observations from Apra (with only the surge component included) because the sea levels recorded during both of these storms fail to exceed 98-percentile threshold established here to define extreme sea levels.

5 Conclusion

The study of long-term changes in the magnitude and frequency of extreme high waters is difficult because of the limitations in the types of sea-level data available to the research community at this time. Historically, tide-gauge observations have served as the principal type of sea-level record used to study fluctuations in mean and extreme water levels; however, the extremes documented by tide gauges may differ in timing and severity when compared against extreme high water events identified using high-frequency observations modified to include the effects of waves on sea level. Thus, analysis of the variations in extreme sea levels should be approached with an awareness of two main limitations: 1) Tide gauges are generally located in areas protected from wave energy, so tide-gauge records do not account for the elevation of sea level due to wave setup, and 2) instruments that have sampling intervals of several minutes to an hour (or greater) may not correctly identify the most extreme sea level. Accounting for wave-driven effects is clearly important for disaster management because the uprush of water onto the shoreline in the form of wave runup is the facet of severe events that presents a direct threat to coastal communities.

Water levels with the effects of waves included into the observations can vary significantly from tidal levels, especially when the waves exceed 2 m; setup and extreme runup contributions to sea level can be as high as 1.5 m (as observed during the passage of Typhoon Man-Yi in July of 2007) during large wave events. Extreme sea levels in Ipan and Pago Bay, located on the southeastern coast of Guam, appear to be associated with the passage of typhoons close to the island (<370 km). Most tropical cyclones approach Guam from the southeast and veer toward the northwest after passing the island. High coastal surges are not necessarily produced by the most intense (or the closest) tropical systems. Extreme high water levels in Apra Harbor, on the western coast of Guam, appear to be concentrated in the months of June, July, and August and may be related to typhoons that pass to the west of Guam or sustained periods of gale-force monsoonal southwesterlies. The analysis here shows that intense tropical cyclones that come very close to Guam or pass directly over the island do not constitute the only systems that coastal managers should be aware of; relatively distant tropical disturbances (e.g., Typhoon Man-Yi) and sustained monsoonal winds (e.g., August 1991 event) may also produce sea level extremes in Guam.

6 References

1. Allan, J. and Komar, P., 2000. Are ocean wave heights increasing in the Eastern North Pacific? Eos Transactions, American Geophysical Union, Vol. 81, No.47.

2. Bernier, N.B. and Thompson, K.R., 2006. Predicting the frequency of storm surges and extreme sea levels in the northwest Atlantic. Journal of Geophysical Research, Vol. 11, C10009, doi:10.1029/2005JC003168.

3. Bindoff, N.L., et al., 2007. Observations: Oceanic Climate Change and Sea Level. In: The Physical Science Basis. Contribution of Working Group I to the Fourth Assessment Report of the Intergovernmental Panel on Climate Change [S. Solomon, et al. (eds.)]. Cambridge University Press, Cambridge, United Kingdom and New York, NY, USA.

4. Bromirski, P.D., Flick, R.E., and Cayan, D.R., 2003. Storminess variability along the California coast: 1858-2000. Journal of Climate, 16(6), 982.

5. Burdick, D., Brown, V., Asher, J., Gawel, M., Goldman, L., Hall et al., 2008. The state of coral reef ecosystems of Guam. NOAA Technical Report.

6. Dillon, C.P. and Andrews, M.J., 1996. Annual Tropical Cyclone Report. Joint Warning Typhoon Center, Guam, Mariana Islands.

7. Dillon, C.P. and Andrews, M.J., 1997. Annual Tropical Cyclone Report. Joint Warning Typhoon Center, Guam, Mariana Islands.

8. Firing, Y.L. and Merrifield, M.A., 2004. Extreme sea level events at Hawaii: Influence of mesoscale eddies. Geophysical Research Letters, Vol.31, L24306, doi:10.1029/2004GL021539, 2004.

9. Furze, P. and Engel, G., 2002. Annual Tropical Cyclone Report. Joint Warning Typhoon Center, Guam, Mariana Islands.

10. Gilmore, R. E., Englebretson, R. E., Handlers, R. G., and Brand, S., 1995. Typhoon Havens Handbook for the Western Pacific and Indian Oceans Change 4 (No. NRL/PU/7543–95-0023-CH-4). NAVAL RESEARCH LAB MONTEREY CA.

11. Graham, N.E. and Diaz, H.F., 2001. Evidence for intensification of North Pacific winter cyclones since 1948. Bulletin of American Meteorological Society 82, 18691893.

12. Gray, W.M., 1968. Global view of the origin of tropical disturbances and storms. Technical paper No. 114.

13. Guard, C., Hamnett, M.P., Neumann, C.J., Lander, M.A., and Siegrist, H.G., 1999. Typhoon vulnerability study for Guam. Water and Environmental Research Institute of the Western Pacific. Technical Report No. 85.

14. Haigh, I., Nicholls, R., and Wells, N., 2010. Assessing changes in extreme sea levels: Application to the English Channel, 19002006. Continental Shelf Research, doi:10.1016/j.csr.2010.02.002.

15. Jensen, J.W., Joeson, J.M.U, and Siegrist, H.G., 1997. Groundwater discharge styles from an uplifted Pleistocene island karst aquifer, Guam, Mariana Islands. In: B.F. Beck and J.B. Stephenson (Editors), The Engineering Geology and Hydrology of Karst Terranes. Balkema, Springfield, Missouri.

16. Lander, M.A., 1994. Description of a monsoon gyre and its effects on the tropical cyclones in the Western North Pacific during August 1991. Weather and Forecasting, Vol. 9, 640-654.

17. Lander, M.A., 1995. Specific tropical cyclone track types and unusual tropical cyclone motions associated with a reverse-oriented monsoon trough int he Western North Pacific. Weather and Forecasting, Vol. 11, 170-186.

18. Lander, M.A., 2004. A rainfall climatology for Saipan: distribution, return-periods, El Niño, tropical cyclones, and long-term variations. Water and Environmental Research Institute of the Western Pacific. Technical Report No. 103.

19. Lowe, R.J., Falter, J.L., Bandet, M.D., Pawlak, G., Atkinson, M.J., Monismith, S.G., Koseff, J.R., 2005. Spectral wave dissipation over a barrier reef. Journal of Geophysical Research, 110, C04001.

20. Lugo-Fernandez, A., Roberts, H.H., Suhayda, J.N., 1998. Wave transformations across a Caribbean fringing-barrier coral reef. Continental Shelf Research 18, 1099-1124.

21. Marcos, M., Tsimplis, M.N., and Shaw, A.G.P., 2009. Sea level extremes in southern Europe, J. Geophys. Res., 114, C01007.

22. Mautner, D.A. and Guard, C.P., 1992. Annual Tropical Cyclone Report. Joint Warning Typhoon Center, Guam, Mariana Islands.

23. McInnes, K.L., O'Grady, J.G., Hubbert, G.D., 2009. Modelling sea level extremes from storm surges and wave setup for climate change assessments in Southeastern Australia. Journal of Coastal Research, SI 56, 1005-1009.

24. Mendez, F.J., Menendez, M., Luceo, A., Losada, I.J., 2006. Estimation of the long-term variability of extreme significant wave height using a time-dependent peak over threshold (POT) model. Journal of Geophysical Research 111, C07024.

25. Menendez, M., Mendez, F.J., Losada, I.J., and Graham, N.E., 2008. Variability of extreme wave heights in the northeast Pacific Ocean based on buoy measurements. Geophysical Research Letters, 35, L22607.

26. Menendez, M., Mendez, F. J., and Losada, I. J., 2009. Forecasting seasonal to interannual variability in extreme sea levels. ICES Journal of Marine Science, 66, 14901496.

27. Menendez, M., and Woodworth, P.L., 2010. Changes in extreme high water levels based on a quasi-global tide-gauge dataset. Journal of Geophysical Research, 115, C10011.

28. Mylroie, J.E., Jenson, J.W., Taborosi, D., Jocson, J.M.U., Vann, D.T., and Wexel, C., 2001. Karst features of Guam in terms of a general model of carbonate island karst. Journal of Cave and Karst Studies 63(1): 9-22.

29. Pugh, D.T., 1987. Tides, surges and mean sea-level: a handbook for engineers and scientists. Wiley, Chichester, 472pp.

30. Pequignet, A.C., Becker, J.M., Merrifield, M.A., Boc, S.J., 2011. The dissipation of wind wave energy across a fringing reef at Ipan, Guam. Coral Reefs, 30, 71-82.

31. Randall, R.H. and Holloman J., 1974. Coastal survey of guam. University of Guam Marine Laboratory, Technical Report 14.

32. Roberts, H.H., Murray, S.P., Suhayda, J.N., 1997. Physical processes in a fore-reef shelf environment. Proceedings, Third International Coral Reef Symposium.

33. Rudolph, D.K. and Guard, C.P., 1991. Annual Tropical Cyclone Report. Joint Warning Typhoon Center, Guam, Mariana Islands.
34. Ruggiero, P., Komar, P.D., Allan, J.C., 2010. Increasing wave heights and extreme value projections: The wave climate of the U.S. Pacific Northwest. Coastal Engineering, 57, 539-532.

35. Stockdon, H.F., Holman, R.A., Howd, P.A., Sallenger, A.H., 2006. Empirical parameterization of setup, swash, and runup. Coastal engineering, 53, 573-588.

36. Taborosi, D., Jensen, J.W., Mylroie, J.E., 2004. Karst Features of Guam Mariana Islands. Water and Environmental Research Institute of the Western Pacific. Technical Report No. 104.

37. Vetter, O., 2007. Setup observations over two fringing reefs: Mokuleia Reef, Oahu and Ipan Reef, Guam. Masters Thesis. University of Hawaii at Manoa. Honolulu, HI.

38. Vetter, O., Becker, J. M., Merrifield, M.A., Pequignet, A.C., Aucan, J., Boc, S.J., and Pollock, C.E., 2010. Wave setup over a Pacific Island fringing reef. Journal of Geophysical Research, 115, C12066.

39. Woodworth, P.L., 2006. Some important issues to do with long-term sea level change. Philosophical Transactions of the Royal Society A, 364, 787-803.

40. Woodworth, P.L., and Blackman, D.L., 2004. Evidence for systematic changes in extreme high waters since the mid-1970s. Journal of Climate, 17(6), 1190-1197.